GHGT-11

Assessing model uncertainties through proper experimental design

Hilde Kristine Hvidevold[a]*, Guttorm Alendal[a,b], Truls Johannessen[c,d], Trond Mannseth[e,a]

[a]University of Bergen, Department of Mathematics, Johannes Brunsgt 12, 5008 Bergen, Norway; [b]Uni Computing, Norway; [c]University of Bergen, Geophysical Institute, Norway; [d]Uni Bjerknes, Norway; [e]Uni CIPR, Norway

Abstract

This paper assesses how parameter uncertainties in the model for rise velocity of CO_2 droplets in the ocean cause uncertainties in their rise and dissolution in marine waters. The parameter uncertainties in the rise velocity for both hydrate coated and hydrate free droplets are estimated from experiment data. Thereafter the rise velocity is coupled with a mass transfer model to simulate the fate of dissolution of a single droplet.

The assessment shows that parameter uncertainties are highest for large droplets. However, it is also shown that in some circumstances varying the temperature gives significant change in rise distance of droplets.

1. Introduction

All models have uncertainties in the model output. These uncertainties originates from different sources, such as uncertainties in input variables, numerical inaccuracy, and uncertainties in model parameters [1]. It is challenging to assess these uncertainties in model output and the challenge increases with model complexity. Still it is important to access these uncertainties to document predictability quality and to quantify model output accuracy.

This can only be achieved by gathering enough in-situ and experimental data for model calibration, including parameter estimation, and validation for the large variety of models being used in risk assessments of CCS. One way to assess and quantify the uncertainty in the estimated parameters is

---

* Corresponding author. Tel. 0047 55584858:.
E-mail address: HildeKristineHvidevold@math.uib.no.

through Linearized Covariance Analysis (LCA) (see for instance [2]). This method can also assist in identifying what kind of additional data that will provide a more robust model and how to design experiments in order to achieve them.

In Hvidevold et al. [3] we addressed the parameter uncertainties in a model for the rise velocity of a hydrate free CO_2 droplet, quantifying the uncertainties in a laboratory experiment and parameter fitting reported in Bigalke et al. [4]. Then we studied experiments with different pressure and density conditions separately. We also made suggestions on how to perform a similar experiment with the objective to reduce these uncertainties. This study takes this a step further: Now we combine all experiments with different pressure and density and find a common uncertainty vector for these, in addition hydrate covered droplets are addressed. The rise velocity model is connected to the other sub-model for predicting CO_2 droplet rise, a mass transfer model [5], [6], [7]. We will focus on simulating the rise of one single droplet, a very simple model consisting of two ordinary differential equations. The scope is to assess how the parameter uncertainties in the rise velocity model influence on the rising distance of a single droplet released at 800 meters.

The numerical model describing the rise and dissolution of a single droplet in seawater can be described by the coupled differential equations

$$\frac{dz}{dt} = u = \left(\frac{8gr(\rho_c - \rho_d)}{3C_d(u)\rho_c} \right)^{1/2} , \tag{1}$$

$$\frac{dm}{dt} = \dot{M} = -2\text{Sh}(u,r)D\pi r(C_s - C_\infty), \tag{2}$$

where we have assumed that there is no horizontal current. The rise velocity of the droplet, u, is dependent on the droplet radius, r, the density of CO_2, ρ_d, and seawater, ρ_c, and the drag coefficient C_d. The mass transfer from the droplet into seawater is driven by concentration differences on the droplet surface C_s and ambient water, C_∞. The Sherwood number, Sh, is a function of the rise velocity and the radius and D is the diffusion coefficient. The Drag coefficient in equation (1), the Sherwood number and the concentration C_s in equation (2) play a key role in the prediction of rise velocity and droplet dissolution. They will in general vary with droplet type and surroundings, and should ideally be estimated from experimental data for each specific case. We will study hydrate coated and hydrate free liquid CO_2 droplets, and need different expressions for C_d, Sh and C_s for each case.

2. Model expressions for hydrate coated and hydrate free CO$_2$ droplets

An introduction to the expression used for the drag coefficient, the Sherwood number and the concentration of the droplet surface C_s for the two models studied here is given below.

2.1. Drag Coefficient

The drag coefficient may be split into the friction factor $f_{h,c}$ and the deformation factor D_f, $C_d = f_{h,c} D_f$. A number of expressions for $f_{h,c}$ and D_f exist. They are generally complex and dependent on several factors [8] [9]. Under the assumption that bubbles attain shapes that minimize their energies, Bigalke et al. [4] derived the following expression for the deformation factor

$$D_f = [2/(3.974 \times 10^{-3}(\text{We-}12.62)^2 - 7.186 \times 10^{-4}(\text{Eo-}17.87)^2$$
$$+ 3.280 \times 10^{-5} \text{ EoWe}((\text{Eo-}27.77)(\text{We-}8.405) + 67.08) + 1.130]^2, \tag{3}$$

where We=$2r\rho_c u^2/\sigma$ and Eo =$g(\rho_c - \rho_d)4r^4/\sigma$ are the Weber number and Etövös number, respectively. Surface tension is denoted σ.

From experimental data Bigalke et al. [4] estimated two expression for the friction factor. For droplets with hydrate coating the friction factor is expressed as

$$f_h = \frac{9}{\sqrt{\text{Re}}} + 0.9\,\frac{0.75\text{Eo}^2}{0.75\,\text{Eo}^2 + 4.5} = \frac{9}{\sqrt{\text{Re}}} + \theta_{h,1}\frac{\text{Eo}^2}{\text{Eo}^2 + \theta_{h,2}}, \tag{4}$$

while the friction factor for hydrate free droplet is

$$f_c = \frac{48}{\text{Re}} + 0.9\,\frac{0.75\text{Eo}^2 + 0.6}{0.75\,\text{Eo}^2 + 14.5} = \frac{48}{\text{Re}} + \theta_{c,1}\frac{\text{Eo}^2 + \theta_{c,2}}{\text{Eo}^2 + \theta_{c,3}}. \tag{5}$$

Where Re=$2r\rho_c u/\mu$ is the Reynolds number, μ is the dynamic viscosity and $\theta_{(c,h),i}$ are parameters estimated by parameter fitting. The subscript h and c denotes hydrate presence or absence, respectively, i=1,2,3. The solution of equation (1) can be written $u=u(x, \boldsymbol{\theta})$, where x represent the experimental conditions, here radius, pressure and temperature. This equation can be used to find an estimate for $\boldsymbol{\theta}$, denoted $\boldsymbol{\theta}^*$, by comparing u for different radiuses, pressure and temperature conditions to corresponding experimental observations, U.

Due to measurement errors $\boldsymbol{\theta}^*$ is not equal to the true parameter vector. Linearized Covariance Analysis (LCA), see e.g. [10], can be used to calculate a region in parameter space that with a given probability level contains the true parameter. This region is called a 100(1 - α)% confidence region, α $\in$ (0,1).

The calculation is based on the assumption that the model is linear with respect to the parameters; this is not the case for our model. However if the nonlinearity is not too severe the LCA results can still be trusted. Therefore the validity of the linearization should be assessed, for this purpose curvature measures of nonlinearity [11] will be used.

Bates and Watts [11] divided between two types of nonlinearity; the nonlinearity due to the parameterization of the model and the intrinsic nonlinearity. These two types of nonlinearity can, through calculations omitted here, be given as scalar values called relative curvature measures. To assess the validity of a particular confidence region calculated with LCA, Bates and Watts [11] suggested to compare the relative curvature measures with an appropriate cut-off value. Let P and I denote scaled parameter effect curvature and scaled intrinsic curvature, respectively, i.e., the relative curvature measures divided by their cut-off values. If the curvatures I or P are above 1 Bates and Watts [11] argued that LCA-based confidence regions should not be trusted. However, this cut-off value does not represent a sharp division between acceptable and unacceptable nonlinearity, see e.g. [12].

2.2. Sherwood number and solubility of CO_2

The Sherwood number can be found through various correlations or can be derived from experimental data. There exists a limited amount of experimental data for mass transfer of CO_2 droplets in seawater. From those experiments that exists, e.g. [13] [14], different models have been derived and suggested, e.g. [15], [16], [17], [5]. Since a direct comparison is difficult, especially in the presence of hydrate, we use the model suggested by Chen et al [7], together with their expression for the solubility of CO_2. Hence, the Sherwood number is

$$\text{Sh}_h = (2 + 0.69\,\text{Re}^{1/2}\,\text{Sc}^{1/3})(1 + 4.6707 \times 10^{-4}\,\text{Re} - 1.1871 \times 10^{-6}\,\text{Re}^2 + 1.4766 \times 10^9\,\text{Re}^3), \tag{6}$$

where the last term is the ratio of total effective droplet area to total area of an equivalent sphere. Solubility of CO2 droplets decrease with decreasing pressure and due to hydrate coating it increase with increasing temperature, in contrast to hydrate free CO_2 droplets [18].

In the hydrate free case we use the Ranz-Marshall correlation [19] to calculate the Sherwood number

$$\text{Sh}_c = 2 + 0.69\,\text{Re}^{1/2}\,\text{Sc}^{1/3}, \tag{7}$$

where Sc=$\mu/D\rho_c$ is the Schmidt number. For the concentration of CO_2 on the droplet surface Teng et al. [20] argumented that dissolution rate of droplets in ocean depends weakly on depth and suggested that constant solubility may be used if an appropriate value is selected.

3. Uncertainties in the rise velocity

In [4] they performed a total of nine experiments with different pressures and temperatures for hydrate free and hydrate coated CO_2 droplets. The pressure and temperature in the experiment varied between 8.3-24.8MPa and 1.9-13.9°C. Assuming that the uncertainties in pressure and temperature conditions are neglectable the standard deviation of the measurement error given in [3] is valid.

We can combine the experiments in the hydrate coated region to calculate an uncertainty for the parameters in equation (4), and the experiments for the hydrate free region to find an uncertainty for the parameters in equation (5). In Table 1 a 95% confidence region, V, for the conducted experiments is shown together with the curvature measures. The relative uncertainty in each parameter, $\theta_{(c,h),i}^{rel}$, is the absolute parameter uncertainty divided by the estimated parameter value.

In [3] we performed a parameter uncertainty analysis and a nonlinearity assessment on the rise velocity of a hydrate free CO_2 droplet for three experiments with fixed pressure and density. We divided the analysis into two groups with slightly different experimental conditions. In both groups the nonlinearity assessment gave I<1. In addition the first group had P>1, while the second group gave P below 1. The assessment made from the LCA results from the first group was very similar to that made from the second group, where P<1. This strengthened our belief in the LCA results from the first group, in particular since the values of P from the results in the first group were not much larger than 1.

Values of P and I related to the LCA results in the current paper is listed in Table 1. Both values of P and one of the I-values are larger than 1, but none of the values are very high. Recalling that the value 1 does not represent a sharp division between acceptable and unacceptable nonlinearity, and based on our previous experience (see, previous paragraph), we continue our investigation using the LCA-results in Table 1. A more thorough investigation of the validity of these LCA-results, like a Monte Carlo study, would be a natural part of further work with these results.

Figure 1 show how the uncertainty in the parameters affect the rise velocity, equation (1), for the hydrate and hydrate free case.

Table 1. Values associated to the LCA 95% confidence region for the experiments. Relative uncertainty of each parameter, $\theta_{(c,h),i}^{rel}$, and confidence regions, V, is shown together with scaled curvatures, n is the total number of measurements.

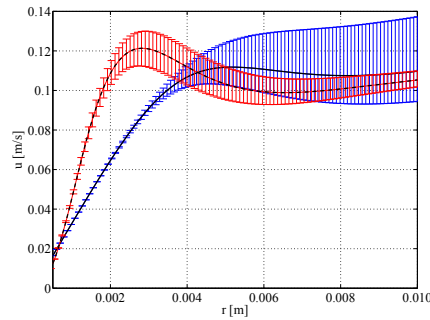| Hydrate coated					Hydrate free						
n	$\theta_{h,1}^{rel}$	$\theta_{h,2}^{rel}$	V	P	I	n	$\theta_{c,1}^{rel}$	$\theta_{c,2}^{rel}$	$\theta_{c,3}^{rel}$	V	P	I
424	0.554	0.003	0.025	3.46	1.33	126	0.199	0.115	0.270	0.009	2.50	0.17

Figure 1: Illustrate how uncertainties in the parameters affect the rise velocity, equation (1), ρ_d=1030.7 and ρ_c=950. The blue and red lines are the deviation for a hydrate coated and a hydrate free droplet, respectively. The black dotted and solid line is the estimated rise velocity for a hydrate free and a hydrate coated droplet, respectively.

4. Simulation of the rise and dissolution of a single CO_2 droplet

The ODE's (1) and (2) is integrated with a 4-5 order Runge-Kutta method to simulate the rise and dissolution of a single CO_2 droplet in seawater. The seawater density and the density if CO_2 is calculated from the Gibbs Seawater (GSW) Oceanographic Toolbox [21], and a 32 term Modified Benedict-Webb-Rubin equation of state [20], respectively. The salinity is set to 34.8 and D = 7.1141×10^{-15}Tk/μ, where Tk is the temperature in Kelvin. The concentration in the ambient water C_∞ is assumed to be zero. All the droplets are released at 800meter. When the droplet diameter is 1mm the simulation stops and we assume that remaining mass is dissolved at the last depth. For each droplet we perform *m* simulations where we pick a set of parameter values within the 95% confidence region, Table 1. In the illustrations the results that differ most from the results when the estimated parameter sets are used is shown. This will correspond to the parameter sets that result in the highest and lowest rise velocity, Figure 1.

For *hydrate free droplets* we use equation (3), (5) and (7) in (1) and (2). The droplets surface concentration, C_s=1363.33 × 44.01g/m^3, is constant [22]. The parameter values in the friction factor, estimated by [4], are given in equation (5) and is denoted $\theta_{c,est}$. Even though hydrate free CO_2 droplets does not exists is seawater for temperatures lower than 10°C, simulations will be done for such temperatures. The model is included to investigate the effect the parameter uncertainty have on rise and dissolution of a single droplet, always keeping in mind that these simulations are strictly theoretical.

Equation (3), (4) and (6) in (1) and (2) is used to simulate *hydrate free droplets*. The droplets surface concentration is calculated with the expression derived in [7]. The parameter values in the friction factor are given in equation (6) and are denoted $\theta_{h,est}$, and the rise velocity using these parameters will be referred to as the estimated rise velocity.

Figure 2a) shows the depth and time span where *hydrate coated droplets* are fully dissolved for five different temperatures. The deviations due to the uncertainty in rise velocity are small, ±3m and ±2.5min from the estimated rise velocity. Figure 1 explains this; the parameter uncertainties have little effect on the rise velocity for droplets smaller than 1cm in diameter. Investigating one temperature; the droplet that dissolves fastest in deepest depth have highest rise velocity, see Figure 4b. The temperature have more impact than the uncertainty in the velocity, if the temperature decreases from one to zero the droplets travels about 20m higher and use 6min longer before being dissolved. This is caused by the temperature dependency on solubility of hydrate coated CO_2 droplets.
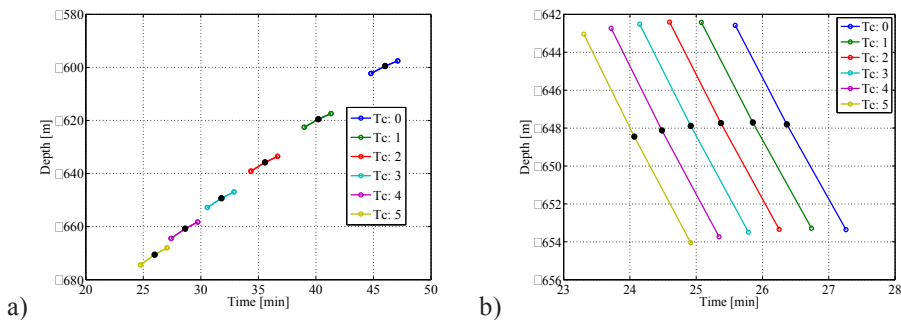
Figure 2: Show when a droplet released at 800m is fully dissolved for different temperatures, Tc, for a) hydrate coated and b) hydrate free droplets. The parameters that mostly affect the rise velocity, colours, are used in addition to $\theta_{(c,h),est}$, black dots. The droplet is initially 1cm in diameter.

The depth and time span where *hydrate free droplets* are fully dissolved for five different temperatures is shown in Figure 2b). The deviations due to the uncertainty in rise velocity is ±(5-6) meter and less than 1 minute from the estimated rise velocity. This is more than for hydrate coated droplet, because there is higher uncertainty affects on smaller droplets, see Figure 1. Here the droplet with the lowest velocity uses longest time to dissolve and travel shortest in the water column.

The total amount of dissolved CO_2, normalized with respect to the initial droplet mass, is plotted against the depth in Figure 3a). It illustrates that the larger the temperature is the more CO_2 dissolves per meter in the lowest depths. After 60 meters about 72% of the droplet is released when the Tc=5°C, yellow, in contrast to 55% for Tc=0°C, blue. The hydrate free droplet, black line, lays somewhere in between, here difference due to temperatures changes is almost invisible and is therefore omitted. From Figure 3b) we note that the difference due to rise velocity uncertainty have little impact on where in the water column the droplet dissolves.

If the initial droplet diameter is 2cm the deviations due to the uncertainty in rise velocity increase, Figure 4a). Now the deviation from the estimated rise velocity is ±(24-40) m and ±(5-9) min due to rise velocity uncertainties. This is because the uncertainty in the rise velocity is large for big droplets, see Figure 1. The difference due to temperature is not that dominant, but is bigger than for smaller droplets.
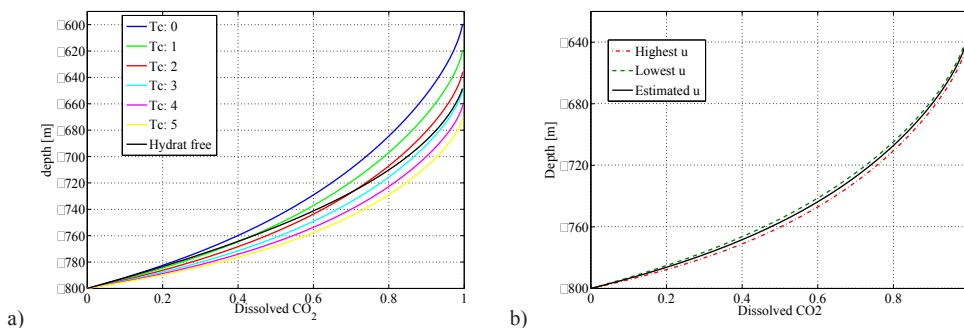

Figure 3: Dissolved CO_2 for droplets with initial diameter 1 cm. In a) colours represent hydrate coated droplets with different temperatures, the black represent a hydrate free droplet. Only the estimated rise velocity is used. In b) Tc = 2°C. The black line represents $\theta_{h, est}$ while the green and red use the two sets that deviates most from the estimated.
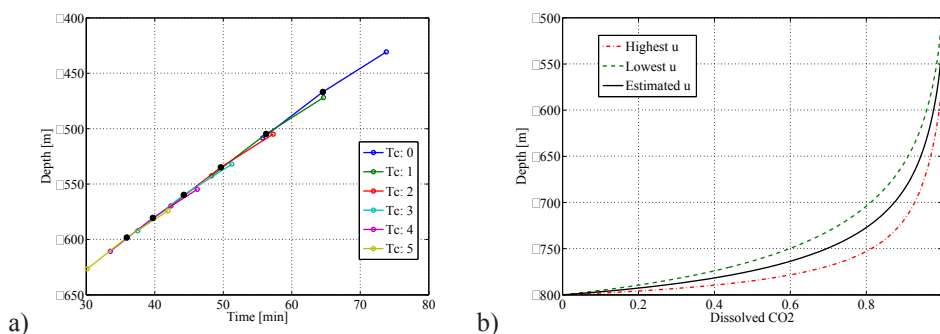
Figure 4: Hydrate coated a) Show when a droplet released at 800m is fully dissolved for different temperatures, Tc. The two parameters that mostly affect the rise velocity are used in addition to $\theta_{h,est}$, black circles. The droplet is initially 2cm in diameter. b) Dissolved CO_2 when Tc=2°C. The green and red are the two sets that deviates most from $\theta_{h,est}$, the black line.

From Figure 4b) we note that the droplet with highest velocity dissolves more CO_2 in the lower water depths compared with the low velocity droplet.

5. Conclusion

The simulations show that the parameter uncertainties in the rise velocity model have little impact on the simulations performed here, especially for small droplets, i.e. close to spherical. Hence the parameters estimated by Bigalke et al. [4] seems to be sufficiently accurate, at least for the pressure and temperature regime studied here.

For hydrate coated CO_2 droplets the variation in temperature appears to have higher influence on the rise height and dissolution of a droplet in the ocean than parameter uncertainties in the rise velocity. However, it seems like the uncertainties associated with the mass transfer for hydrate coated droplets are higher and dominate the rise intervals obtained.

The models used are based on experimental data at pressures higher than 800 meter. This is not necessarily representative for shallower marginal seas, like the North Sea, where the natural and seasonal temperature variations are higher than in the deep ocean. The challenge is to predict the impact on marine waters from CO_2 release and dissolution at such depths. For this experimental and in-situ data at appropriate depths will be vital for model calibration and validation.

Acknowledgements

References

[1] Oberkampf, W. L. and Roy, C. J. *Verification and validation in scientific computing*, Cambridge University Press; 2010.

[2] Seber, G. A. F. and Wild, C. J. *Nonlinear regression*, Wiley-Interscience; 2003.

[3] Hvidevold, H. K., Alendal, G., Johannessen, T. and Mannseth, T., Assessing model parameter uncertainties for rising velocity of CO_2 droplets through experimental design, *International Journal of Greenhouse Gas Control* 2012; **11** (0): 283-289.

[4] Bigalke, N. K., Enstad, L. I., Rehder, G. and Alendal, G., Terminal velocities of pure and hydrate coated CO_2 droplets and CH_4 bubbles rising in a simulated oceanic environment, *Deep Sea Research Part I: Oceanographic Research Papers* 2010; **57** (9): 1102-1110.

[5] Gangstø, R., Haugan, P. M. and Alendal, G., Parameterization of drag and dissolution of rising CO_2 drops in seawater, *Geophys. Res. Lett* 2005; **32** (L10612.

[6] Alendal, G. and Drange, H., Two-phase, near-field modeling of purposefully released CO_2 in the ocean, *Journal of geophysical research* 2001; **106** (C1): 1085-1096.

[7] Chen, B., Song, Y., Nishio, M. and Akai, M., Large-eddy simulation of double-plume formation induced by CO_2 dissolution in the ocean, *Tellus B* 2003; **55** (2): 723-730.

[8] Kelbaliyev, G. I., Drag coefficients of variously shaped solid particles, drops, and bubbles, *Theoretical Foundations of Chemical Engineering* 2011; **45** (3): 248-266.

[9] Clift, R., Grace, J. R. and Weber, M. E. *Bubbles, drops, and particles*, Dover Publications; 2005.

[10] Aster, R. C., Borchers, B. and Thurber, C. H. *Parameter estimation and inverse problems*, Academic Press; 2012.

[11] Bates, D. M. and Watts, D. G., Relative curvature measures of nonlinearity, *Journal of the Royal Statistical Society. Series B (Methodological)* 1980; **42** (1): 1-25.

[12] Grimstad, A. A., Kolltveit, K., Mannseth, T. and Nordtvedt, J. E., Assessing the validity of a linearized accuracy measure for a nonlinear parameter estimation problem, *Inverse Problems* 2001; **17** (5): 1373-1390.

[13] Brewer, P. G., Peltzer, E. T., Friederich, G. and Rehder, G., Experimental determination of the fate of rising CO_2 droplets in seawater, *Environmental science & technology* 2002; **36** (24): 5441-5446.

[14] Ogasawara, K., Yamasaki, A. and Teng, H., Mass transfer from CO_2 drops traveling in high-pressure and low-temperature water, *Energy & fuels* 2001; **15** (1): 147-150.

[15] Ozaki, M., Minamiura, J., Kitajima, Y., Mizokami, S., Takeuchi, K. and Hatakenaka, K., CO_2 ocean sequestration by moving ships, *Journal of Marine Science and Technology* 2001; **6** (2): 51-58.

[16] Hirai, S., Okazaki, K., Tabe, Y., Hijikata, K. and Mori, Y., Dissolution rate of liquid CO_2 in pressurized water flows and the effect of clathrate films, *Energy* 1997; **22** (2): 285-293.

[17] Mori, Y. H. and Mochizuki, T., Dissolution of liquid CO_2 into water at high pressures: A search for the mechanism of dissolution being retarded through hydrate-film formation, *Energy conversion and management* 1998; **39** (7): 567-578.

[18] Aya, I., Yamane, K. and Nariai, H., Solubility of CO_2 and density of CO_2 hydrate at 30 MPa, *Energy* 1997; **22** (2): 263-271.

[19] Crowe, C. T., Schwarzkopf, J. D., Sommerfeld, M. and Tsuji, Y. *Multiphase flows with droplets and particles*, CRC press; 2011.

[20] Teng, H., Masutani, S. M., Kinoshita, C. M. and Nihous, G. C., Solubility of CO_2 in the ocean and its effect on CO_2 dissolution, *Energy conversion and management* 1996; **37** (6): 1029-1038.

[21] McDougall, T. J. and Barker, P. M., Getting started with TEOS-10 and the Gibbs Seawater (GSW) Oceanographic Toolbox, *SCOR/IAPSO WG* 2011; **127** (1-28.

[22] Thorkildsen, F. and Haugan, P. M., Numerical model for plumes of dissolving CO_2 droplets in seawater. 1993, The Nansen Environmental and Remote Sensing Center.